Frequency Power Spectrum of Temperature Fluctuations in Free Convection

Xiao-Zhong Wu, Leo Kadanoff, Albert Libchaber, and Masaki Sano[(a)]
The James Franck and The Enrico Fermi Institutes, The University of Chicago, 5640 South Ellis Avenue, Chicago, Illinois 60637
(Received 4 January 1990)

The behavior of power spectra in a Rayleigh-Bénard convection experiment in a helium-gas cell is reported. The high-frequency part of the data for all Rayleigh numbers from 7×10^6 to 4×10^{14} is fit by a single functional form, obtained by a natural generalization of a multifractal analysis. Low-frequency data cannot be fit in this form.

PACS numbers: 47.25.Cg, 44.25.+f, 47.25.Qv

During the last few years, a series of studies have been conducted of free thermal convection in low-temperature helium gas.[1-5] The wide range of Rayleigh numbers enables one to study different turbulent states and the evolution of various statistical quantities, for example, the Nusselt number, the histogram of local temperature fluctuations, and the mean velocity field. However, the frequency power spectrum of local temperature fluctuations has not been studied systematically in the whole range of Rayleigh numbers. (This power spectrum is the squared magnitude of the time Fourier transformation of the temperature fluctuations measured by a given bolometer.) Power spectra have always been an important aspect of turbulence study, but mostly in wave numbers.[6-9] One of the key results arising from the Kolmogorov[6] theory of turbulence is that the wave-number power spectrum has the form

$$P(k)=k^{-5/3}g(k/k_d)\,, \tag{1}$$

where g is a universal function. This result is described as a result of a cascade of kinetic energy to shorter wavelengths followed by dissipation at short distances. Here the dissipation wave number k_d is expected to vary as a power of the Reynolds number. However, except for situations in which the frozen-flow hypothesis[10] is reasonable, not very much is known about the relationship between wave-number and frequency power spectra.

The main spirit of the experiment has already been described in previous reports.[2,3,5] In this paper, we present results from a new cell of a diameter 20 cm and height 40 cm. With this cell, we can reach Rayleigh numbers up to 1×10^{15}. The cell is filled with helium gas at a given pressure and operated at about 5 K. The cell is heated from below by a dc power input and the temperature of its top plate is regulated. The temperature fluctuations at various points within the cell are measured by bolometers as As-doped Si cubes of about 0.2 mm. The control parameter in this experiment is the Rayleigh number R, which is defined as

$$R=\alpha g L^3\Delta/\nu\kappa\,, \tag{2}$$

where α is the thermal expansion coefficient, g is the gravitational acceleration, L is the height of the cell, Δ is the measured temperature drop across the cell, and ν and κ are the kinematic viscosity and the thermal diffusivity of the helium gas, respectively.

For a small-aspect-ratio cell, the flow in the center region of the cell is homogeneous and is believed to be characteristic of free convection flow. Therefore we shall focus our discussion on the frequency power spectrum $P(\omega)$ for the temperature fluctuation signal at the center of the cell. The high-frequency end of each power spectrum is cut off by noise at about 10^2 Hz and the frequency range is about 3 decades. In the discussion below, the frequency ω will be given in unit of κ/L^2, and the power spectrum $P(\omega)$ will be normalized so that its frequency integral is one.

Figure 1 shows a series of power spectra at Rayleigh numbers ranging from 7×10^6 to 4×10^{14}. The region at very low frequency reflects the motion of the largest scales. The flatness of the power spectra at low frequencies may be interpreted as a manifestation of a cutoff at the size of the cell. In the region of the previously introduced soft turbulence[8] ($R<10^8$), the power spectrum drops sharply with frequency immediately after the flat region. The lack of a power law between the flat and the

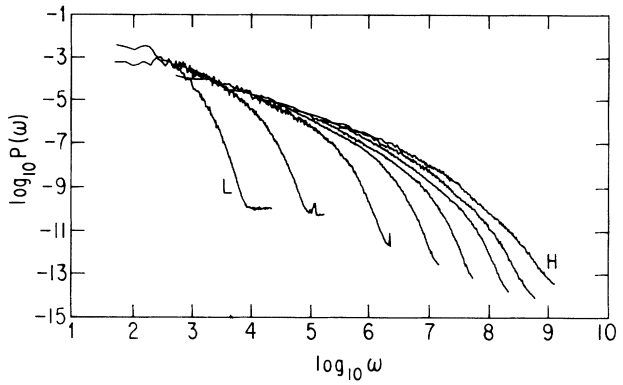

FIG. 1. The power spectra in a log-log scale for $R=7.0\times10^6$, 1.1×10^8, 4.0×10^9, 7.3×10^{10}, 6.0×10^{11}, 6.7×10^{12}, 4.1×10^{13}, and 4.3×10^{14}. The curves L and H are for the lowest and highest R, respectively. ω is in units of κ/L^2.

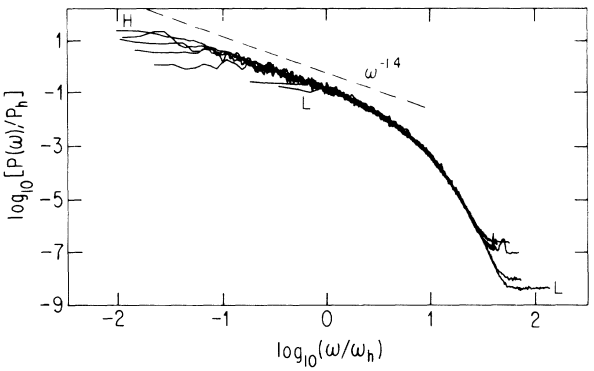

FIG. 2. $\log_{10}[P(\omega)/P_h]$ vs $\log_{10}(\omega/\omega_h)$ for $R=7.0\times10^6$, 2.1×10^7, 1.1×10^8, 6.0×10^8, 4.0×10^9, 2.5×10^{10}, and 7.3×10^{10}. The curve L and H are for the lowest and highest R, respectively.

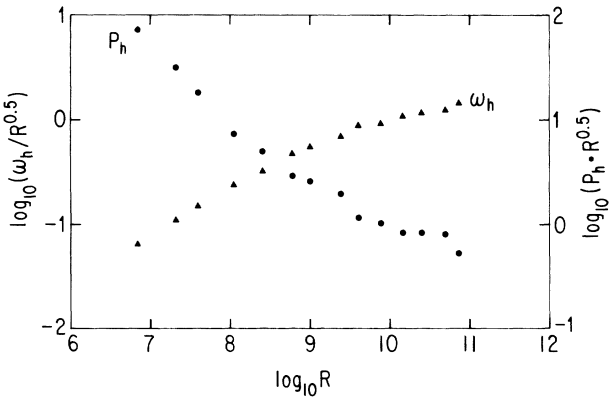

FIG. 3. A log-log plot of $\omega_h/R^{0.5}$ and $P_hR^{0.5}$ vs the Rayleigh number. ω_h and P_h have been calculated from the slope and the intercept of the straight line in the $\log[P(\omega)]$ vs $\omega^{0.55}$ plot. The X coordinate is chosen as $\omega_h/R^{0.5}$ to compare ω_h with ω_p, which varies as $R^{0.5}$. The Y coordinate is chosen accordingly.

sharp drop region suggests there is no inertial cascade. The whole spectrum, except for the flat region, can be described as

$$P(\omega)=P_h\exp[-(\omega/\omega_h)^{\beta}], \tag{3}$$

where P_h, ω_h, and β are parameters ($\beta=0.55\pm0.05$).

As the Rayleigh number increases above 10^8 and into the hard turbulence regime,[2] the tails of the power spectrum still retain the shape defined by Eq. (3) up to $R=7\times10^{10}$. This similarity in the tails makes it attractive for us to plot those power spectra together, with their high-frequency part superposed, and study how the lower-frequency part evolves with Rayleigh number. Figure 2 is a plot of $\log_{10}[P(\omega)/P_h]$ vs $\log_{10}(\omega/\omega_h)$ for seven different Rayleigh numbers between 7×10^6 and 7×10^{10}. Figure 3 shows the dependence of ω_h and P_h in Eq. (3) upon R. Note that the power spectra in Fig. 2 are superposed by a relative translational transformation, i.e., a shift of $\log_{10}(\omega_h)$ along the X axis and a shift of $\log_{10}(P_h)$ along the Y axis. All the power spectra exhibit the very same high-frequency behavior. Moreover, the straight-line region of the power spectra shows that there is a power law developed between the flat low-frequency cutoff and the sharp drop at high frequencies. The exponent of the power law is -1.4 ± 0.05, which is surprisingly the same as the $-\frac{7}{5}$ predicted by Bolgiano[7] and Obukhov[8] for the wave-number power spectrum in thermal stratification. Changes in the Rayleigh number change only the range of this power law. The difference between the regimes of hard turbulence ($R>10^8$) and soft turbulence ($R<10^8$) is that the range of the power law is almost zero in the latter case. As shown in Fig. 3, ω_h increases faster than $R^{0.5}$ at low Rayleigh numbers and approaches $R^{0.5}$ as the Rayleigh number goes to 7×10^{10}. On the other hand, the characteristic frequency ω_p for the low-frequency cutoff is known[2,3] to vary as $R^{0.5}$. The dependence of ω_h and ω_p on the Rayleigh number is consistent with the fact shown in Fig. 2, that the range of the power law increases with the Rayleigh number, and saturates as the Rayleigh number reaches 7×10^{10}.

Thus, the power spectrum $P(\omega)$ for $R\leq7\times10^{10}$ can be represented by a scaling form akin to that of Eq. (1):

$$P(\omega)=P_h\exp[f(\omega/\omega_h)]. \tag{4}$$

The decay of the power for high frequencies, which must be a result of the dissipation of the turbulent motion, can be described by Eq. (3). A power law with an exponent of about -1.4 appears at lower frequencies. Thus, these parts of the data show a scaling behavior.

As the Rayleigh number increases above 7×10^{10}, the range of the -1.4 power law saturates. But now the data reduction of Fig. 2 no longer works, since the form of the high-frequency part of the power spectrum is no longer independent of Rayleigh numbers. Figure 4(a) shows power spectra for Rayleigh numbers between 7×10^{10} and 4×10^{14}; after a relative translational transformation, it is clear that the different spectra have quite different curvature. The specific transformation in Fig. 4(a) is chosen for the best illustration. However, there is once again a simple way to bring all these high-Rayleigh-number data together. Figure 4(b) shows that all these power spectra collapse under the following transformation:[11] Take the vertical axis as

$$f=\frac{\log[P(\omega)/P_0]}{\log(R/R_0)} \tag{5a}$$

and the horizontal axis as

$$\alpha=\frac{\log(\omega/\omega_0)}{\log(R/R_0)}, \tag{5b}$$

where R_0, P_0, and ω_0 are Rayleigh-number-independent

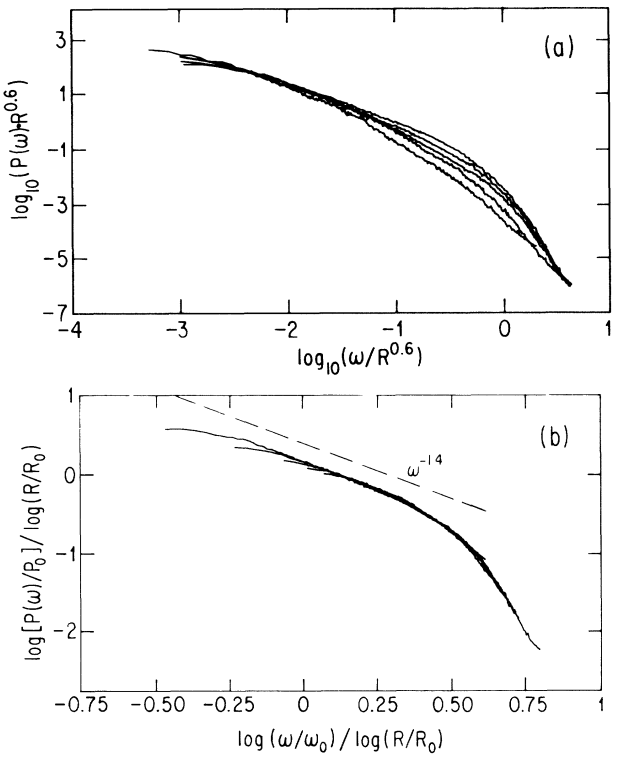

FIG. 4. (a) $\log_{10}[P(\omega)R^{0.6}]$ vs $\log_{10}(\omega/R^{0.6})$ and (b) $\log[P(\omega)/P_0]/\log(R/R_0)$ vs $\log(\omega/\omega_0)/\log(R/R_0)$ for $R=7.3\times10^{10}$, 6.0×10^{11}, 6.7×10^{12}, 4.1×10^{13}, and 4.3×10^{14}. The lowest R data in (a) is the up curve, and in (b) the curve spanning the whole range.

parameters which are chosen as

$$R_0=1\times10^8,\quad P_0=(5.8\pm0.7)\times10^{-7},$$

$$\omega_0=(1.1\pm0.2)\times10^5.$$

The most important parameter among the three is R_0, which decides how much the curve, at a given Rayleigh number, should be bent under this transformation. P_0 and ω_0 merely determine the relative positions of each curve. Since the transformation depends on $\log(R_0)$, it is not very sensitive to R_0. R_0 being any value between 8×10^7 and 8×10^8 leads to good superposition, but $R_0=1\times10^8$ is slightly better. It is interesting that R_0 is about the Rayleigh number of the transition from soft to hard turbulence in this system. This data reduction is invariant under the change of P_0 to $P_0(R/R_0)^\gamma$ and ω_0 to $\omega_0(R/R_0)^\beta$, since this only leads to a change of the common origin. γ and β are zero in the transformation (5a) and (5b)

We conclude that there is also a simple relation among the power spectra taken in the range $R>7\times10^{10}$. The data suggest the possibility of a universality in the plots of f vs α for different Rayleigh numbers. But notice that because of the limited dynamical range of the data, the larger the Rayleigh number, the smaller the range on Fig. 4(b) covered by the power spectrum. So we cannot be sure that the apparent universality of the plots shown in Fig. 4(b) will really carry out at very large Rayleigh numbers.

So far, our description of the experimental results above show there are two regimes, one for $R\le7\times10^{10}$ with a generic relation between $\log[P(\omega)/P_h(R)]$ and $\log[\omega/\omega_h(R)]$, and another for $R\ge7\times10^{10}$ with a generic relation between $\log[P(\omega)/P_0]$ divided by $\log(R/R_0)$ and $\log(\omega/\omega_0)$ divided by $\log(R/R_0)$. However, they can be combined into one overall relation between a generalized f and α defined by

$$f=\frac{\log[P(\omega)/P_h]}{S},\tag{6a}$$

$$\alpha=\frac{\log(\omega/\omega_h)}{S},\tag{6b}$$

where S is a scale factor for logarithmic frequency intervals. For $R\le7\times10^{10}$, S is a constant of $\log(7\times10^{10}/1\times10^8)$, and P_h and ω_h have the values given in Fig. 3. For $R\ge7\times10^{10}$, $S=\log(R/R_0)$, and we take $P_h=P_0\times(R/R_0)^\gamma$, $\omega_h=\omega_0(R/R_0)^\beta$, where γ and β may be chosen to match the values of P_h and ω_h of $R\le7\times10^{10}$. With these choices of parameters, we can fit all the data in the entire range of Rayleigh numbers by a single function $f(\alpha)$: Since the power spectrum for $R=7\times10^{10}$ fall equally well on Figs. 2 and 4(b), which are for two different regions of Rayleigh numbers, the two curves must be identical, within the experimental error. Figure 5 is part of the combined f-α plot.

To reveal more about this multifractal, let us imagine the cascade from a given low frequency to higher frequency. This cascade will induce an attenuation of the amplitude of the power spectrum. Assume that as the frequency is raised from ω to $\omega+d\omega$ the power is attenuated by an amount proportional to the change in the logarithmic frequency interval via

$$P(\omega+d\omega)=P(\omega)\left[1-\frac{d\omega}{\omega}g(\alpha)\right],\tag{7}$$

where α is given by Eq. (6b). The basic assumption is that α is an appropriate measure of the frequency intervals in which a universal form of attenuation might occur. Then the integral of Eq. (7) gives

$$P(\omega)=P_0\exp\left[-\int_{\omega_1}^{\omega}\frac{d\omega'}{\omega'}g\left(\frac{\log(\omega'/\omega_h)}{S}\right)\right],\tag{8}$$

where P_0 is a constant, ω_1 stands for a certain low frequency, and the ω_h is a parameter. If the integral of $g(\alpha)$ with respect to α is $-f(\alpha)$, then Eq. (8) implies our result

$$P(\omega)=P_h\exp\left[Sf\left(\frac{\log(\omega/\omega_h)}{S}\right)\right].\tag{9}$$

We expect the function $f(\alpha)$ to be independent of the

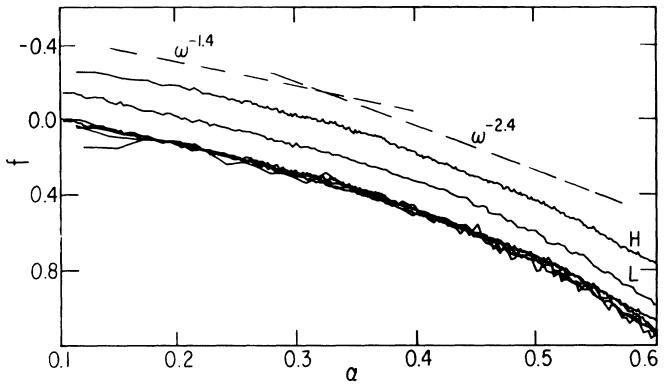

FIG. 5. f-α plot for data of $R=2.1\times10^{7}$, 1.1×10^{8}, 7.3×10^{10}, 6.7×10^{12}, and 4.3×10^{14}. The origin of the coordinates is shifted to be the same as that of Fig. 4(b). The curve L of $R=7.3\times10^{10}$ and H of 4.3×10^{14} are also shifted arbitrarily along the Y axis to compare with the two power laws.

Rayleigh number, but ω_h, P_h, and S may be Rayleigh-number dependent.

However, it seems that for $R>10^{14}$, the power spectrum tends to develop a second power law with an exponent -2.4 ± 0.1 at higher frequencies. In the magnified f-α plot, Fig. 5, two power laws are compared with the power spectra. If there were two power laws, this would contradict the multifractal fit for this range of Rayleigh number. However, we cannot sharply distinguish between the multifractal possibility and the two power laws since the high-Rayleigh-number data are squeezed to a small piece of the f-α plot under the transformation (6a) and (6b). From our reading of Fig. 5, there are two options: Either the multifractal property of the power spectrum is the asymptotic one for very large Rayleigh number, or it is an intermediate property as the power spectrum develops from one power law to two power laws. Maybe we are seeing the first hints of a new regime of turbulence arising above $R=10^{14}$. We need to reach higher Rayleigh numbers and attain a larger dynamical range before we can sharply distinguish between these possibilities.

Yakhot[12] has shown how much of the data from the smaller cell[2-4] could be rather well fitted by a slow crossover between two power-law regimes. These earlier data can also be fitted by the multifractal analysis described above, with the very same f vs α.

In conclusion, we have fitted the high-frequency part of the power spectra for all Rayleigh numbers from 7×10^{6} to 4×10^{14} by a single functional form, obtained by a natural generalization of a multifractal analysis. The low-frequency data are not included in this form. Perhaps, on one hand, this fitting might be considered to be indicative of a remarkable universality which appears in the highly dissipative part of convective turbulence. If so, we might foresee an interesting generalization of Kolmogorov's picture of turbulence. On the other hand, the fits are not perfect; for example, there are three adjustable parameters for the spectra at low Rayleigh numbers (i.e., P_h, ω_h, and a low-frequency cutoff), and the experimental data for very high Rayleigh numbers covers only a small range of the f-α curve. The physical significance to $R=7\times10^{10}$, which marks the division between the two curve fits, is not understood. Furthermore, our theoretical discussion introduces the scale of frequency in a rather *ad hoc* fashion. It may well be that the apparently good fits give a deceptive view of the processes involved. We do not know.

We would like to thank Lei Wu, Victor Yakhot, Anton Kast, and Gianluigi Zanetti for very helpful discussions. This research has been supported by the University of Chicago, Materials Research Laboratory; the experimental work is also supported by NSF under Grant No. DMR-8722714.

[a]Permanent address: The Research Institute of Electrical Communication, Tohoku University, Sendai 980, Japan.

[1]D. C. Threlfall, Ph.D. thesis, University of Cambridge, 1976 (unpublished); J. Fluid Mech. **67**, 17 (1975).

[2]F. Heslot, B. Castaing, and A. Libchaber, Phys. Rev. A **36**, 5870 (1987).

[3]B. Castaing, G. Gunaratne, F. Heslot, L. Kadanoff, A. Libchaber, S. Thomae, X. Z. Wu, S. Zaleski, and G. Zanetti, J. Fluid Mech. **204**, 1 (1989).

[4]X. Z. Wu, B. Castaing, F. Heslot, and A. Libchaber, in *Universalities in Condensed Matter,* edited by R. Jullen *et al.*, Springer Proceeding in Physics Vol. 32 (Springer-Verlag, Berlin, 1988), p. 208.

[5]M. Sano, X. Z. Wu, and A. Libchaber, Phys. Rev. A **40**, 6421 (1989).

[6]A. N. Kolmogorov, C. R. Acad. Sci. U.S.S.R. **30**, 301 (1941).

[7]R. Bolgiano, J. Geophys. Res. **64**, 2226 (1959).

[8]A. M. Obukhov, Dokl. Akad. Nauk S.S.S.R. **125**, 1246 (1959).

[9]A. S. Monin and A. M. Yaglom, *Statistical Fluid Mechanics* (MIT Press, Cambridge, MA, 1975), Vol. 2.

[10]G. I. Taylor, Proc. Roy. Soc. London A **164**, 476 (1938).

[11]These are the familiar variable transformation used in multifractal analysis of turbulence data. See B. Mandelbrot, J. Fluid Mech. **62**, 331 (1974); U. Frisch and G. Parisi, in *Turbulence and Predictability in Geophysical Fluid Dynamics and Climate Dynamics,* edited by M. Ghil, R. Benzi, and G. Parisi (North-Holland, Amsterdam, 1985), p. 84; D. Lovejoy and S. Schertzer, in "Fractals," edited by L. Pietronero (Plenum, New York, to be published). B. Castaing has proposed a particular example of a result of this type [J. Phys. (Paris) **50**, 147 (1989)]. In all of these references, the transformed variables were velocity and wave number.

[12]V. Yakhot (private communication).